J Mol Model (2012) 18:4739–4744
DOI 10.1007/s00894-012-1455-7

ORIGINAL PAPER

In silico evaluation of TERT inhibition by anticancer drugs

Porika Mahendar · Kalam Sirisha · Umasankar Kulandaivelu · Prakhya Laxmi Jaya Shankar · Tippani Radhika · Abbagani Sadanandam

Received: 6 March 2012 / Accepted: 30 April 2012 / Published online: 6 June 2012
© Springer-Verlag 2012

Abstract The activation of telomerase represents an early step in carcinogenesis. Increased telomerase expression in malignant tumors suggests that telomerase inactivation may represent a potential chemotherapeutic target. In this work, existing anticancer drugs were docked against telomerase reverse transcriptase (TERT) using a Lamarckian genetic algorithm (LGA). Autodock's scoring function was applied to each of the molecules in order to identify the inhibitor with the strongest pharmacological action. The structural insights provided by this study regarding binding poses and possible interactions, free energies of binding, and drug scores aided in the identification of potential inhibitory compounds. The ranks of the various ligands investigated were based on the final docked energy values. Among nine selected compounds, vindesine, temsirolimus, and cyclosporine were found to be more potent TERT inhibitors than the standard inhibitor, curcumin.

Keywords Cancer · Docking · 3DU6 · TERT · Telomerase inhibition

P. Mahendar · T. Radhika · A. Sadanandam (✉)
Department of Biotechnology, Kakatiya University,
Warangal 506 009 Andhra Pradesh, India
e-mail: nandamas@rediffmail.com

K. Sirisha · U. Kulandaivelu
Medicinal Chemistry Research Division,
Vaagdevi College of Pharmacy,
Warangal 506 001 Andhra Pradesh, India

P. L. J. Shankar
Department of Bioinformatics, Alpha Arts and Science College,
Chennai, India

Introduction

Cancer is a generic term for a group of over 100 chronic diseases that can affect any part of the body. A defining feature of cancer is the rapid creation of abnormal cells that grow beyond their usual boundary and can invade adjoining parts of the body. The cells may also spread to other organs, a process referred to as metastasis. It is expected that the annual incidence of cancer will increase steadily to 15 million new cases in the year 2020 [1]. Thus, the challenge of developing a novel method to treat cancer is becoming increasingly significant.

A common hallmark of human cancers is the overexpression of telomerase, a ribonucleoprotein complex that is responsible for maintaining the length and integrity of chromosome ends [2, 3]. Telomeres are present at the ends of eukaryotic chromosomes, which consist of an array of tandem repeats of a nucleotide, 5′-TTAGGG-3′ [4]. Telomerase protects the chromosomes from degradation and repair activities, and are therefore essential for ensuring chromosome stability [5]. Telomerase is responsible for adding telomeric DNA repeats onto the 3′-ends of chromosomes. It plays a pivotal role in cellular immortalization and carcinogenesis [6]. Telomere elongation counterbalances the natural shortening of linear chromosomes due to the end-replication problem, preventing senescence, apoptosis, and genome instability [7]. Telomere stabilization by telomerase can lead to unlimited cell proliferation. A deficiency in telomerase function leads to a limited renewal capacity for highly proliferative cells. Telomere length deregulation and telomerase activation is an early, and perhaps necessary, step in cancer cell evolution. Previous studies have shown that telomerase activity is present in 85–90 % of human tumors, but not in adjacent normal cells, which makes telomerase a good target not only for cancer diagnosis but also for the development of novel therapeutic agents [8].

Telomerase consists of two major subunits: telomerase RNA (TR) and telomerase reverse transcriptase (TERT), as well as telomerase-associated proteins [9, 10]. In contrast to TR, which is commonly expressed in both normal tissues (which lack telomerase activity) and cancers, TERT is highly expressed in tumor cells [11–13]. The high concentration of TERT in almost all cancer cells, the dependency of most cancer cells on TERT activity, and the scarcity of TERT in most normal cells suggest that TERT would be a good target for cancer treatment. Therefore, targeting this catalytic subunit represents a promising approach for diminishing telomerase function that will probably not cause substantial side effects on telomerase-negative or somatic cells. The inhibition of TERT activity by a specific inhibitor induces growth arrest and apoptosis of cancer cells. Therefore, the discovery and development of specific TERT inhibitors would provide this tempting prospect in anticancer research.

Thus, in a continuation of our work on telomerase and more specifically TERT [14, 15], herein we describe studies of the molecular docking of currently marketed anticancer drugs (Fig. 1) onto the crystal structure of TERT with a view to evaluating them as TERT inhibitors. The differences in their binding modes were investigated. Curcumin, a well-known TERT inhibitor, was employed as a standard [16–21]. *Tribolium castaneum* (red flour beetle) TERT was chosen for the present study, as this domain showed the highest similarity with human TERT [22–25]. On the basis

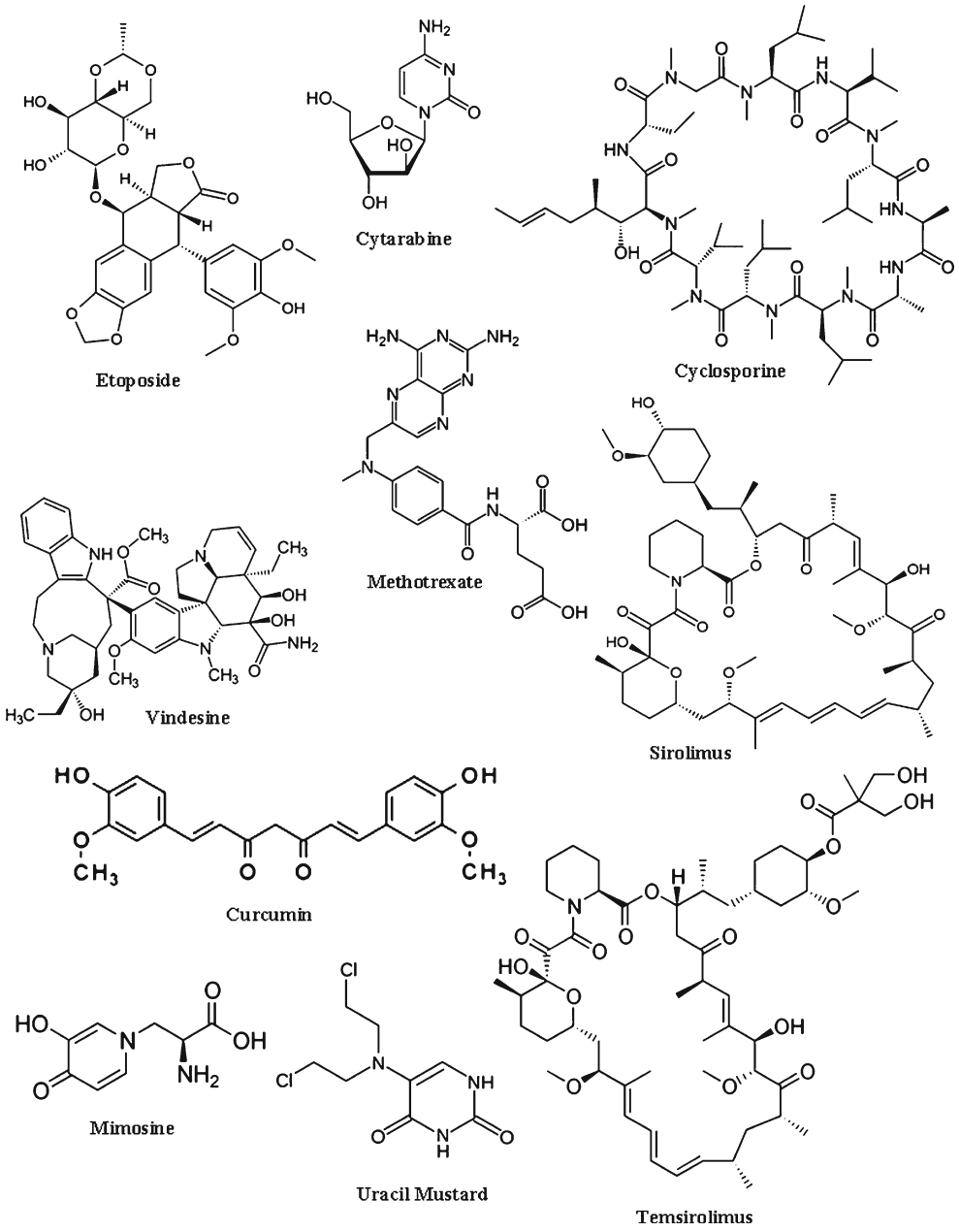

Fig. 1 Chemical structures of the anticancer drugs (ligands)

of the docking results, the anticancer drugs were ranked to identify inhibitor(s) specific for the enzyme TERT.

Materials and methods

Preparation of ligand structures

The ligands used in this study were downloaded from DrugBank [26]. The ligands downloaded in MOL/SDF format were first converted to the Protein Data Bank (PDB) format using Open Babel [27]. Each ligand was checked for polar hydrogens and assigned atom types (AD4), partial atomic charges (with the Gasteiger method), rotatable bonds, and atomic solvation parameters, and then saved in pdbqt format. In addition to amide and ring torsions, all of the torsions were released for flexible ligands. The real challenge during docking is to use flexible ligand molecules; that is, those with rotatable torsion angles. The partial charges of the nonpolar hydrogens were added to the charges of the carbons they were bonded to, and were deleted afterwards. The atom type for the aromatic carbons was reassigned so that it would be handled by the aromatic carbon grid map.

Protein molecule retrieval and preparation

The molecular docking program Autodock 4.0 was used to determine the potential binding modes between the currently marketed anticancer drugs and the selected enzyme target, *Tribolium castaneum* TERT. The Lamarckian genetic algorithm was applied to analyze protein–ligand interactions. A Solis–Wets local search was performed for energy minimization. The docked structures of the ligands were generated after a reasonable number of evaluations.

The crystal structure of *Tribolium castaneum* TERT (Fig. 2) was retrieved from the RCSB Protein Data Bank (PDB ID: 3DU6) [28]. To prepare the enzyme so that it is suitable for docking studies, the PDB structure 3DU6 was processed in the graphical software AutoDockTools. Using the default setting in Autodock Tools, polar hydrogen atoms were added and fixed, and then the atoms were typed as per the rules in AutoDock. The Gasteiger charges were calculated and assigned to the atoms of the structure. The coordinates as well as the charge and solvation information for the receptor were added and utilized for further docking studies.

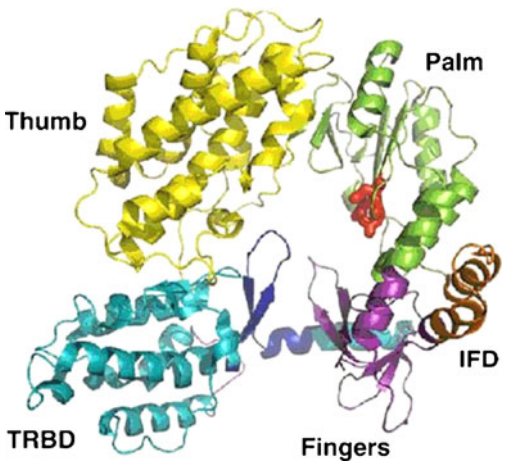

Fig. 2 High-resolution structure of *Tribolium castaneum* TERT

Protein–ligand docking

Grid-box generation

The grid parameter file of the protein was generated using Auto Dock Tool. A grid box was generated that was large enough to cover the entire protein binding site and allow all ligands to move freely. The number of grid points in the x, y and z directions were 60×60×60 points, and a spacing of 0.375 Å was employed. A three-dimensional grid was created by the AutoGrid4 algorithm to evaluate the binding energies between the ligands and the proteins. The Lennard–Jones parameters 12–10 and 12–6 (supplied with the software package) were used to model H-bonds and van der Waals interactions, respectively. The distance-dependent dielectric permittivity of Mehler and Solmajer [29] was used to calculate the electrostatic grid maps. The center of the ligand in the X-ray crystal structure was used as the center of the grid box. For protein structures that did not have ligands in the binding site, the center of the binding site was estimated from the structure and taken as the center of the grid box.

Optimal size of the grid box

The grid box covered the entire binding site, and the volume of the grid box allowed the binding of ligands to extend beyond the actual binding site, with nonspecific binding into adjacent pockets. At this stage, the protein was fixed into the three-dimensional grid, and a probe atom was placed at each grid point. The affinity and electrostatic potential grid were calculated for each type of atom in the ligand. The free energy of a particular ligand configuration was found through the trilinear interpolation of the affinity values and electrostatic interactions of the eight grid points surrounding each atom in the ligand. Reducing the grid-box size would significantly reduce the CPU time needed for the docking calculation, an important consideration for drug discovery. The optimal grid-box size allowed approximately two-thirds of the ligand molecule to occupy the target binding site, with the remaining one-third able to bind with adjacent pockets. Larger grid boxes provide the optimal balance between the number of screening ligands and the CPU time required for docking.

Table 1 Docking results for the anticancer molecules on 3DU6

Name of ligand	Docked energy (kcal/mol)	Estimated free energy of binding(kcal/mol)	Rank order
Cyclosporine	−10.74	−5.36	3
Cytarabine	−7.09	−6.64	6
Etoposide	−6.76	−6.32	7
Methotrexate	−5.31	−4.17	9
Mimosine	−7.71	−7.01	5
Sirolimus	−8.33	−6.91	4
Temsirolimus	−10.80	−6.98	2
Uracil mustard	−5.60	−4.06	8
Vindesine	−12.39	−13.3	1
Curcumin	−8.62	−5.71	

Ligand docking

AutoDock 4.0 and a Lamarckian genetic algorithm (LGA) [30] were used for protein-fixed ligand-flexible docking calculations. A series of docking parameters were set up. Not only the atom types but also the generations and the number of runs for the LGA were edited and properly assigned according to the requirements of the Amber force field. Ten search attempts were performed for each ligand with a population size of 150 individuals, a maximum number of 2,500,000 energy evaluations, a mutation rate of 0.02, a crossover rate of 0.80, and an elitism value of 1. The maximum number of generations of the LGA run before termination was 27,000. Other docking parameters were set to the software's default values, and 2710 runs were set. After docking, the ligands were ranked according to their final docked energies calculated during the docking procedure from the sum of the intermolecular energy and the internal energy of the ligand.

Results and discussion

3DU6 and the ligands (curcumin, cyclosporine, cytarabine, etoposide, methotrexate, uracil mustard, temsirolimus, sirolimus, vindesine, and mimosine) were subjected to docking

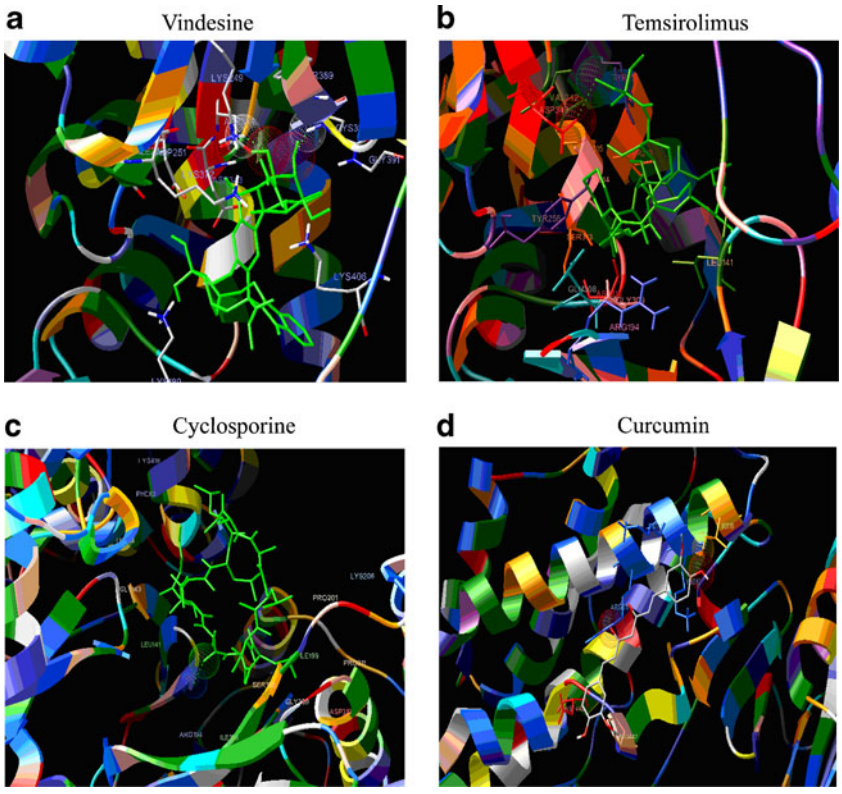

Fig. 3 Modeling the molecular docking of the ligands with telomerase (3DU6)

analysis using Autodock 4.0. According to previous studies on 3DU6 [23–25], 26 amino acid residues were identified at the active site: Gly182, Lys189, Arg194, Pro201, Asp202, Ser203, Ala204, Phe209, Leu220, Tyr224, Lys225, Thr226, Ser227, Lys249, Ile252, Arg253, Asp254, Gly308, Ala322, Gly314, Asp325, Ile338, Arg340, Asp344, Asn369, and Gly391. As most of the amino acid residues at the active site are hydrophobic, they are the main contributors to the receptor–ligand interaction. The protein was further manipulated by adding Kollman partial charges and solvent parameters. Like the protein, the structures of the ligands were also prepared by deleting their nonpolar hydrogen atoms and adding Mulliken atomic charges obtained from Gaussian03. The LGA implemented in the Autodock program was applied. The most representative binding modes of the ten conformations calculated, with at least one hydrogen bond to one of the catalytic aspartates, were chosen for analysis. When the simulations had completed, the docked structures were analyzed and the interactions were noted. The final docked energy, hydrogen-bond interactions, and the binding distance between the donor and acceptor were measured to identify the best conformers.

After studying several docking poses, the complex that formed with the least energy and with the top rank was chosen based on the final docked energy of the stable conformation. Rank lists were collected from the docking log file. The minimum free energy of binding estimated for each docking process was a measure of the affinity of the inhibitor for the active site of the 3DU6 (Table 1).

The results indicate that some of the docked molecules exhibited good binding interactions with the active site of 3DU6. The estimated free energy of binding was found to range from −13.3 to −4.17 kcal mol^{-1} across all ligands. The standard drug, curcumin, exhibited a docked energy of −8.62 kcal mol^{-1}. Vindesine, with its relatively low docked energy (−12.39 kcal mol^{-1}), was found to exhibit a strong interaction with 3DU6, and was found to be the most potent molecule (top ranked) among all the ligands. This molecule displayed two hydrogen-bond interactions: one at the residue Asp344 and the other at Cys390 (Fig. 3a), in addition to hydrophobic, van der Waals, and π–π interactions. After vindesine, temsirolimus (Fig. 3b), with a docked energy of −10.8 kcal mol^{-1}, and cyclosporine (Fig. 3c), with a docked energy of −10.74 kcal mol^{-1}, exhibited the next highest interaction energies with 3DU6, and were thus ranked second and third, respectively. These three molecules were found to be more potent than curcumin, as they were found to bind 3DU6 (TERT) more effectively than curcumin (Fig. 3d) and thus to inhibit it in the order vindesine > temsirolimus > cyclosporine. Further, sirolimus was found to be almost as potent as curcumin, with a docked energy of −8.33 kcal mol^{-1}. The other molecules were also ranked according to their docked energies, but were found to be less potent than the curcumin standard.

Conclusions

A total of nine drug molecules were evaluated for their TERT inhibitory activities. Among them, vindesine, temsirolimus, and cyclosporine were found to be more potent than the standard inhibitor, curcumin. The successful location of global minima for the TERT protein by genetic algorithms may lead to significant changes in the way in which drug development is performed. The continued development of novel drugs will likely be at the forefront of cancer therapy, and this work is intended to provide a synopsis of anti-TERT approaches that may revolutionize cancer therapeutics in the future. Hence, potential inhibitors of TERT and valuable anticancer agents with higher binding affinities and bioavailability but less toxicity could be obtained by optimizing the structures of these drugs in this manner. Further, this work could be extended to perform an experimental study of how these drugs inhibit TERT protein and hence reduce telomere elongation and arrest the cell cycle at different phases in humans.

Acknowledgments Mahendar Porika is thankful to the University Grants Commission (UGC), New Delhi, India, for the award of a Junior Research Fellowship and a Senior Research Fellowship.

References

1. WHO (2003) Global cancer rates could increase by 50 % to 15 million by 2020. World Health Organization, Geneva. http://www.who.int/mediacentre/news/releases/2003/pr27/en/
2. Shay JW, Zou Y, Hiyama E, Wright WE (2001) Telomerase and cancer. Hum Mol Genet 10:677–685
3. Pacini F, Cantara S, Capezzone M, Marchisotta S (2011) Telomerase and the endocrine system. Nat Rev Endocrinol 7:420–430
4. Kumaki F, Takeda K, Yu ZX, Moss J, Ferrans VJ (2002) Expression of human telomerase reverse transcriptase in lymphangioleiomyomatosis. Am J Respir Crit Care Med 166:187–191
5. Martínez P, Blasco MA (2011) Telomeric and extra-telomeric roles for telomerase and the telomere-binding proteins. Nat Rev Cancer 11:161–176
6. Xie M, Mosig A, Qi X, Li Y, Stadler PF, Chen JJ (2008) Structure and function of the smallest vertebrate telomerase RNA from teleost fish. J Biol Chem 283:2049–2059
7. Xie M, Podlevsky JD, Qi X, Bley CJ, Chen JJ (2010) A novel motif in telomerase reverse transcriptase regulates telomere repeat addition rate and processivity. Nucleic Acids Res 38:1982–1996
8. Han M, Chen JL, Hu Y, He CL, Shuai WP, Yu JH, Chen HL, Liang WQ, Mayumi T, Shinsaku N, Gao JQ (2008) In vitro and in vivo tumor suppressive activity induced by human telomerase transcriptase-targeting antisense oligonucleotides mediated by cationic liposomes. J Biosci Bioeng 106:243–247
9. Kaufer BB, Arndt S, Trapp S, Osterrieder N, Jarosinski KW (2011) Herpesvirus telomerase RNA (vTR) with a mutated template

sequence abrogates herpesvirus-induced lymphomagenesis. PLoS Pathog 7:e1002333
10. Sun PM, Wei LH, Luo MY, Liu G, Wang JL, Mustea A, Könsgen D, Lichtenegger W, Sehouli J (2007) The telomerase activity and expression of hTERT gene can serve as indicators in the anti-cancer treatment of human ovarian cancer. Eur J Obstet Gynecol Reprod Biol 130:249–257
11. Chang JT, Chen YL, Yang HT, Chen CY, Cheng AJ (2002) Differential regulation of telomerase activity by six telomerase subunits. Eur J Biochem 269:3442–3450
12. Saretzki G (2009) Telomerase, mitochondria and oxidative stress. Exp Gerontol 44:485–492
13. Kraemer K, Fuessel S, Schmidt U, Kotzsch M, Schwenzer B, Wirth MP, Meye A (2003) Antisense-mediated hTERT inhibition specifically reduces the growth of human bladder cancer cells. Clin Cancer Res 9:3794–3800
14. Porika M, Tippani R, Mohammad A, Bollam SR, Panuganti SD, Abbagani S (2011) Evaluation of serum human telomerase reverse transcriptase as a novel marker for cervical cancer. Int J Biol Markers 26:22–26
15. Porika M, Tippani R, Bollam SR, Panuganti SD, Thamidala C, Abbagani S (2011) Serum human telomerase reverse transcriptase: a novel biomarker for breast cancer diagnosis. Int J Clin Oncol 16:617–622
16. Lee JH, Chung IK (2010) Curcumin inhibits nuclear localization of telomerase by dissociating the Hsp90 co-chaperone p23 from hTERT. Cancer Lett 290:76–86
17. Cui SX, Qu XJ, Xie YY, Zhou L, Nakata M, Makuuchi M, Tang W (2006) Curcumin inhibits telomerase activity in human cancer cell lines. Int J Mol Med 18:227–231
18. Hsin IL, Sheu GT, Chen HH, Chiu LY, Wang HD, Chan HW, Hsu CP, Ko JL (2010) N-acetyl cysteine mitigates curcumin-mediated telomerase inhibition through rescuing of Sp1 reduction in A549 cells. Mutat Res 688:72–77
19. Chakraborty S, Ghosh U, Bhattacharyya NP, Bhattacharya RK, Roy M (2006) Inhibition of telomerase activity and induction of apoptosis by curcumin in K-562 cells. Mutat Res 596:81–90
20. Aravindan N, Veeraraghavan J, Madhusoodhanan R, Herman TS, Natarajan M (2011) Curcumin regulates low-linear energy transfer γ-radiation-induced NFκB-dependent telomerase activity in human neuroblastoma cells. Int J Radiat Oncol Biol Phys 79:1206–1215
21. Anand P, Sundaram C, Jhurani S, Kunnumakkara AB, Aggarwal BB (2008) Curcumin and cancer: an "old-age" disease with an "age-old" solution. Cancer Lett 267:133–164
22. Gillis AJ, Schuller AP, Skordalakes E (2008) Structure of the *Tribolium castaneum* telomerase catalytic subunit TERT. Nature 455:633–637
23. Liu XH, Liu HF, Shen X, Song BA, Bhadury PS, Zhu HL, Liu JX, Qi XB (2010) Synthesis and molecular docking studies of novel 2-chloro-pyridine derivatives containing flavone moieties as potential antitumor agents. Bioorg Med Chem Lett 20:4163–4167
24. Liu XH, Liu HF, Chen J, Yang Y, Song BA, Bai LS, Liu JX, Zhu HL, Qi XB (2010) Synthesis and molecular docking study of novel coumarin derivatives containing 4,5-dihydropyrazole moiety as potential antitumor agents. Bioorg Med Chem Lett 20:5705–5708
25. Liu XH, Ruan BF, Liu JX, Song BA, Jing LH, Li J, Yang Y, Zhu HL, Qi XB (2011) Design and synthesis of N-phenylacetyl (sulfonyl) 4,5-dihydropyrazole derivatives as potential antitumor agents. Bioorg Med Chem Lett 21:2916–2920
26. Wishart D, Knox C, Law V (2012) DrugBank (open data drug and drug target database). http://www.drugbank.ca
27. O'Boyle NM, Banck M, James CA, Morley C, Vandermeersch T, Hutchison GR (2011) Open Babel: an open chemical toolbox. J Cheminform 3:33
28. Gillis AJ, Schuller AP, Skordalakes E (2008) PDB: structure of the catalytic subunit of telomerase, TERT. http://www.rcsb.org/pdb/explore/explore.do?structureId=3DU6
29. Mehler EL, Solmajer T (1991) Electrostatic effects in proteins: comparison of dielectric and charge models. Protein Eng 4:903–910
30. Morris GM, Goodsell DS, Halliday RS, Huey R, Hart WE, Belew RK, Olson AJ (1998) Automated docking using a Lamarckian genetic algorithm and an empirical binding free energy function. J Comput Chem 19:1639–1662